Relevance of CD6–Mediated Interactions in T Cell Activation and Proliferation

Article *in* The Journal of Immunology · September 2004

Impact Factor: 4.92 · DOI: 10.4049/jimmunol.173.4.2262 · Source: PubMed

9 authors, including:

Maria Calvo
University of Barcelona
62 PUBLICATIONS **1,454** CITATIONS
SEE PROFILE

María Mittelbrunn
Hospital 12 de Octubre
53 PUBLICATIONS **2,092** CITATIONS
SEE PROFILE

Carlos Enrich
University of Barcelona
172 PUBLICATIONS **4,396** CITATIONS
SEE PROFILE

Francisco Lozano
Hospital Clínic de Barcelona
172 PUBLICATIONS **3,590** CITATIONS
SEE PROFILE

Relevance of CD6-Mediated Interactions in T Cell Activation and Proliferation[1]

Idoia Gimferrer,* Maria Calvo,† María Mittelbrunn,§ Montse Farnós,* Maria Rosa Sarrias,* Carlos Enrich,‡ Jordi Vives,* Francisco Sánchez-Madrid,§ and Francisco Lozano[2]*‡

CD6 is a cell surface receptor expressed on immature thymocytes and mature T and B1a lymphocytes. The ultimate function of CD6 has not been deciphered yet, but much evidence supports a role for CD6 in T cell activation and differentiation. In this study, we show that a fraction of CD6 molecules physically associates with the TCR/CD3 complex by coimmunoprecipitation, cocapping, and fluorescence resonance energy transfer experiments. Image analysis of Ag-specific T-APC conjugates demonstrated that CD6 and its ligand, activated leukocyte cell adhesion molecule (CD166), colocalize with TCR/CD3 at the center of the immunological synapse, the so-called central supramolecular activation cluster. The addition of a soluble rCD6 form significantly reduced the number of mature Ag-specific T-APC conjugates, indicating that CD6 mediates early cell-cell interactions needed for immunological synapse maturation to proceed. This was in agreement with the dose-dependent inhibition of CD3-mediated T cell proliferation induced by soluble rCD6. Taken together, our data illustrate the important role played by the intra- and intercellular molecular interactions mediated by CD6 during T cell activation and proliferation processes. ***The Journal of Immunology*****, 2004, 173: 2262–2270.**

The central event in T cell activation is the interaction of the TCR complex with the Ag peptide presented by the MHC of APC. However, sustained T cell activation requires signal amplification by accessory molecules (1). The immunological synapse (IS)[3] (1) organizes and segregates adhesion molecules and TCR-associated components into two major compartments (2). These areas, referred to as supramolecular activation clusters (SMACs), include the central SMAC (cSMAC), which is enriched in TCR/CD3 complexes and costimulatory molecules (CD4, CD2, and CD28), and the peripheral SMAC (pSMAC), which includes LFA-1 and other adhesion molecules (3, 4). APC surface components are also integral to these clusters, such that MHC-peptide complexes are found in the cSMAC, and ICAM-1, the LFA-1 counterreceptor, is concentrated at the pSMAC. The stability of the IS depends on an intact actin cytoskeleton, the participation of intracellular transport mechanisms, and the accumulation of costimulatory receptors at the T-APC interface, which then increases the overall amplitude and duration of the T cell signaling (5).

CD6 is a surface receptor expressed on thymocytes, mature T cells, the B1a B cell subset, and certain regions of the brain (6, 7). The extracellular region of CD6 is composed of three scavenger receptor cysteine-rich (SRCR) domains, thus including CD6 among the members of the SRCR superfamily of protein receptors (7, 8). The ultimate function of CD6 has not been deciphered yet, but several lines of evidence support a role for CD6 in T cell activation and differentiation. CD6 acts as a costimulatory molecule synergizing with TCR or CD28 to enhance T cell proliferation (9, 10). Although the signaling pathway used by CD6 is mostly unknown, it has been shown that CD6 is tyrosine phosphorylated after stimulation with CD3 alone or by cocross-linking CD3 with CD2 or CD4 (11, 12).

The use of a chimerical CD6 protein (human CD6-Ig) allowed the identification of a CD6 ligand of 100 kDa, designated as CD166 or activated leukocyte cell adhesion molecule (ALCAM) (13). ALCAM/CD166 is an adhesion molecule belonging to the Ig superfamily. It is expressed on mitogen-activated PBMC, and a number of T, B, and monocytic tumor-derived cell lines, as well as on neurons and thymic epithelial cells (14). The CD6-ALCAM/CD166 interaction has been shown to mediate thymocyte-thymic epithelial cell adhesion, which is compatible with a role of CD6 in the development and differentiation of T cells in the thymus (15).

In this study, we present evidence indicating that a fraction of CD6 is physically associated with the TCR/CD3 complex, and that CD6 and its ligand ALCAM/CD166 colocalize with the TCR/CD3 complex at the cSMAC. Furthermore, an important role of CD6 in

*Servei d'Immunologia, Hospital Clínic i Provincial de Barcelona, Institut de Investigacions Biomèdiques August Pi i Sunyer, Barcelona, Spain; †Serveis CientificoTècnics and ‡Departament de Biologia Cel · lular, Institut de Investigacions Biomèdiques August Pi i Sunyer, Facultat de Medicina, Universitat de Barcelona, Barcelona, Spain; and §Servicio de Inmunología, Hospital de la Princesa, Universidad Autónoma de Madrid, Madrid, Spain

Received for publication September 29, 2003. Accepted for publication June 2, 2004.

The costs of publication of this article were defrayed in part by the payment of page charges. This article must therefore be hereby marked *advertisement* in accordance with 18 U.S.C. Section 1734 solely to indicate this fact.

[1] This work was supported by a grant from Ministerio de Ciencia y Tecnología (SAF 2001-1832). M.F. and M.C. are recipients of fellowships from Institut de Investigacions Biomèdiques August Pi i Sunyer and Fondo de Investigaciones Sanitarias-Institut de Investigacions Biomèdiques August Pi i Sunyer, respectively. I.G. is the recipient of a fellowship from Hospital Clínic (Premio Fin de Residencia Emili Letang) and Ministerio de Sanidad y Consumo-Institut de Investigacions Biomèdiques August Pi i Sunyer (Contrato post-formación sanitaria especilaizada). The costs of publication of this article were defrayed in part by the payment of page charges. This article must therefore be hereby marked advertisement in accordance with 18 U.S.C. Section 1734 solely to indicate this fact.

[2] Address correspondence and reprint requests to Dr. Francisco Lozano, Servei d'Immunologia, Hospital Clínic i Provincial de Barcelona, Villarroel 170, Barcelona 08036, Spain. E-mail address: lozano@ub.edu

[3] Abbreviations used in this paper: IS, immunological synapse; ALCAM, activated leukocyte cell adhesion molecule; cSMAC, central SMAC; Cy3, cyanine 3; DC, dendritic cell; DIC, differential interference contrast; E_a, apparent efficiency of FRET; FRET, fluorescence resonance energy transfer; FRET^c, corrected FRET; GAMIg, goat anti-mouse Ig; HEK, human embryonic kidney; MTOC, microtubule-organizing center; PLL, poly(L-lysine); pSMAC, peripheral SMAC; ROI, region of interest; rsCD5/CD6, soluble rCD5/CD6; RT, room temperature; SAv, streptavidin; SEB, staphylococcal enterotoxin B; SEE, staphylococcal enterotoxin E; SMAC, supramolecular activation cluster; SRCR, scavenger receptor cysteine rich; TR, Texas Red.

0022-1767/04/$02.00

T cell-mediated responses is deduced from the inhibitory properties of soluble rCD6 (rsCD6) on IS maturation and T cell proliferation.

Materials and Methods

Cells

PBL were obtained from peripheral blood samples subjected to centrifugation on a standard Ficoll gradient ($d = 1077$). Thymocytes were obtained by disruption of human thymus specimens from children undergoing cardiac surgery. The human T cell lines HUT-78, the lymphoblastoid B cell line Raji, and the erythromyeloid cell line K562 were obtained from the American Type Culture Collection (ATCC, Manassas, VA). The CD5- and CD6-negative 2G5 cells were obtained by FACS and further cloning of Jurkat cells, as reported elsewhere (16). Cell lines were grown in RPMI 1640 with 10% FCS, 1 mM sodium pyruvate, 2 mM L-glutamine, 50 U/ml penicillin G, and 50 μg/ml streptomycin. The human embryonic kidney epithelial cell line HEK 293-EBNA (Invitrogen Life Technologies, Paisley, U.K.) was grown in DMEM/F12 (Invitrogen Life Technologies), supplemented with 100 U/ml penicillin, 100 μg/ml streptomycin, 250 μg/ml geneticin (G418), and 10% FCS. To ease protein purification, serum-free DMEM/F12 medium was used at certain culture stages.

Abs and reagents

The mAbs Cris-1 (anti-CD5, IgG2a), 148.1C3 (anti-CD43, IgG2a), 33-2A3 (anti-CD3ϵ, IgG2a), and 161.8 (anti-CD6, IgG1) were produced by R. Vilella (Hospital Clínic, Barcelona, Spain). The rabbit polyclonal anti-CD3ζ serum was kindly provided by B. Alarcón (Centro de Biología Molecular Severo Ochoa, Universidad Autónoma de Madrid) (17). The anti-ICAM-1 mouse mAb (18) was from F. Luscinskas (Brigham and Women's Hospital and Harvard Medical School, Boston, MA). The mouse MAE1-C10 mAb was provided by F. Sánchez-Madrid (Hospital de la Princesa, Madrid, Spain) (19). Alexa Fluor 488-labeled goat anti-mouse Ig (GAMIg) serum, Rhodamine Red-X-labeled streptavidin (SAv), and goat anti-rabbit serum were obtained from Molecular Probes (Eugene, OR). Affinity-purified Leu-1 (anti-CD5, IgG2a) mAb was purchased from BD Biosciences (Mountain View, CA), and the W6/32 (anti-HLA class I, IgG2a) mAb was from the ATCC (HB-95). FITC-labeled anti-CD5 (UCTH2, IgG1), anti-CD6 (M-T605, IgG1), and anti-CD3 (UCHT1, IgG1) mAbs were from BD Pharmingen (San Diego, CA). FITC-conjugated anti-α-tubulin mAb DM 1A was from Sigma-Aldrich (St. Louis, MO). The 148.1C3 mAb was conjugated to FITC (Sigma-Aldrich), as previously described (20). The Leu-1 and 33-2A3 mAbs were conjugated to cyanine 3 (Cy3) using the Cy3 mAb labeling kit (Amersham Biosciences, Little Chalfont, U.K.). Cy3-conjugated GAMIg were from Sigma-Aldrich. HRP-conjugated SAv was from DakoCytomation (Glostrop, Denmark). Texas Red (TR)-SAv and Tri-color-SAv were from Caltag Laboratories (Burlingame, CA). The generation of rabbit polyclonal antisera against the extracellular region of human CD5 and the intracellular region of CD6 has been reported elsewhere (21, 22). Biotinylation of mAbs and cell surface proteins was performed with EZ-Link sulfo-normal human serum-L chain-L chain biotin, following the manufacturer's instructions (Pierce, Rockford, IL). Mowiol 488 was from Calbiochem (La Jolla, CA), and poly(L-lysine) (PLL) was from Sigma-Aldrich. Staphylococcal enterotoxin E (SEE) and B (SEB) and recombinant human fibronectin were from Toxin Technology (Sarasota, FL). The fluorescent cell tracker chloromethyl derivative of aminocoumarin was from Molecular Probes.

CD6 expression constructions

The expression construct coding for a CD6 form devoid of its 55 C-terminal residues (CD6.A613^{stop}) was obtained by cloning *Sal*I/*Eco*RI- and *Eco*RI/*Bam*HI (Fermentas MBI)-restricted fragments corresponding to the extracellular and cytoplasmic regions of CD6, respectively, into the *Sal*I/*Bam*HI-restricted pHβAPr-1-*neo* mammalian expression vector. The extracellular portion of CD6 was obtained by PCR amplification of the CD6-PB1 cDNA (23) with the 5′-TCTCGTCGACATGTGGCTCTTCTTCGGGAT-3′ and 5′-AACTTCTTTGGGGATGGTGATGGG-3′ primers. The intracellular region of CD6 was obtained by PCR amplification of HUT-78 cDNA with the 5′ GTCACTATAGAATCTTCTGTG-3′ and 5′-GTTGGATCCCTATGCT GAAAAGGCTGGCTGG-3′ primers, the latter introducing a premature stop at position A613. Underlining indicates the positions of restriction sites in the primers.

Immunoprecipitation

Surface-biotinylated cells were lysed for 30 min on ice in a buffer containing 10 mM Tris-HCl, pH 7.6, 140 mM NaCl, 5 mM EDTA, 140 mM NaF, 0.4 mM orthovanadate, 5 mM pyrophosphate, 1 mM PMSF, protease inhibitor mixture tablets (Complete; Boehringer Mannheim, Mannheim, Germany), and 1% of either Nonidet P-40 (Boehringer Mannheim), Brij 96 (Fluka, Buchs, Switzerland), or Brij 58 (Sigma-Aldrich). After centrifugation at 12,000 $\times$ *g* for 15 min at 4°C, the solubilizates were precleared by end-over-end rotation with 50 μl of 50% protein A-Sepharose CL-4B beads (Amersham Biosciences). Immunoprecipitations were conducted by adding 3 μg of specific mAb plus 20 μl of 50% protein A-Sepharose beads, followed by rotating for 2 h at 4°C. The immune complexes were washed three times in lysis buffer with 1% detergent. For reprecipitation, the immune complexes were boiled for 5 min in lysis buffer containing 3% SDS. The eluate was recovered and diluted 9-fold with lysis buffer, and then precleared with 50 μl of 50% protein A-Sepharose beads for 30 min. Proteins were reprecipitated with 5 μl of polyclonal anti-CD6 rabbit antiserum plus 20 μl of protein A-Sepharose beads for 90 min at 4°C. Reprecipitates were washed three times with 200 μl of lysis buffer, eluted by boiling for 5 min in SDS-sample buffer, and run on 8% SDS-PAGE.

For immunodepletion experiments, surface-biotinylated PBL were lysed with 1% Brij 58, and then sequentially immunoprecipitated with anti-CD5 (Cris-1) mAb plus protein A-Sepharose. CD5-depleted and nondepleted lysates were precleared with 50 μl of 50% protein A-Sepharose beads for 30 min before immunoprecipitation with anti-CD3 mAb. After preclearing again with protein A-Sepharose, immune complexes were next reprecipitated with 5 μl of rabbit polyclonal antisera to either anti-CD6 or anti-CD5.

Western blot analysis

Samples resolved by 8% SDS-PAGE were electrophoretically transferred (at 0.4 A, 100 V for 1 h) to nitrocellulose membranes (Bio-Rad, Richmond, CA). Filters were blocked for 30 min at 37°C with 5% nonfat milk powder in PBS, and then incubated for 30 min at room temperature with a 1/1000 dilution of HRP-SAv in blocking solution. After three washes with PBS plus 0.1% Tween 20, the membranes were developed by chemiluminescence with SuperSignal West Dura Extended Duration Substrate (Pierce) and exposure to X-OMAT films (Kodak, Rochester, NY).

Capping assays

All procedures were performed at 4°C, unless otherwise indicated. A total of 1×10^6 PBLs was incubated for 10 min with saturating amounts of biotinylated anti-CD6 (161.8) mAb. After washing with ice-cold PBS, cells were incubated with saturating amounts of TR-SAv for 10 min. For capping to proceed, cells were then incubated at 37°C for 30 min. The reaction was stopped by adding ice-cold PBS plus 0.1% sodium azide. The cells were next transferred onto PLL-coated coverslips and stained for 30 min with FITC-conjugated anti-CD3 (33-2A3) or anti-CD43 (148.1C3) mAbs before fixation with PBS plus 2% paraformaldehyde for 10 min at room temperature (RT). After washing twice, the coverslips were transferred onto Mowiol-treated glass slides, and visualized in a confocal spectral microscope (Leica Microsystems, Mannheim, Germany). The images were analyzed with the Image Processing Leica Confocal Software and Photoshop 4.0 (Adobe Systems, San Jose, CA).

Fluorescence resonance energy transfer (FRET) measurements

A total of 1×10^6 PBLs (in 300 μl of PBS) was transferred onto PLL-coated coverslips for 30 min at RT. After blocking with 1% heat-inactivated rabbit serum for 10 min at RT, cells were incubated for 15 min at 4°C with saturating amounts of FITC (donor)- and Cy3 (acceptor)-labeled Abs, either alone or mixed. Cells were then rinsed twice with cool PBS, and fixed with PBS plus 2% paraformaldehyde for 10 min at RT. After washing twice, the coverslips were transferred onto Mowiol-treated glass slides. For FRET measurement under capping formation, 1×10^6 PBLs were blocked with 1% heat-inactivated rabbit serum for 10 min at RT, and then incubated for 10 min at 4°C with saturating doses of Cy3-labeled or unlabeled anti-CD3 mAb cross-linked with GAMIg. For capping to proceed, cells were incubated for 30 min at 37°C, and then stopped by washing with cool PBS/0.01% azide. Next, cells were transferred onto PLL-coated coverslips and incubated for 15 min at 4°C with saturating amounts of FITC-labeled mAbs, as described above.

FRET measurements were based on the sensitized emission method (24, 25), with minor modifications. A Leica TCS SL laser-scanning confocal spectral microscope (Leica Microsystems) equipped with argon and green HeNe lasers, $\times$100 oil immersion objective lens, and triple dichroic filter (488/543/633 nm) was used. To measure FRET, three images were acquired in all experiments in the same order through the: 1) FITC channel (Absorbance, 488 nm, Emission, 500–555 nm), 2) FRET channel (Absorbance, 488 nm, Emission, 590–700 nm), and 3) Cy3 channel (Absorbance, 543 nm, Emission, 590–700 nm). Background was subtracted from images

before FRET calculations. Control and experiment images were taken under the same conditions of photomultiplier gain, offset, and pinhole aperture. The crossover of donor and acceptor fluorescence through the FRET filter is a constant proportion between the fluorescence intensity levels of donor and acceptor and their bleed-through. To calculate the spectral bleed-through of the donor and acceptor through the FRET filter, images of cells labeled only with FITC-conjugated mAb and cells labeled only with Cy3-conjugated mAb were also taken under the same conditions as for the experiments. The fraction of bleed-through of FITC (A) and Cy3 (B) fluorescence through the FRET filter channel was calculated for different labeling conditions and situations. For capping conditions: FITC anti-CD43, 0.11 ± 0.011; FITC anti-CD6, 0.10 ± 0.01; FITC anti-CD5, 0.11 ± 0.01; and Cy3 anti-CD3, 0.54 ± 0.03. Corrected FRET ($FRET^c$) was calculated on a pixel-by-pixel basis for the entire image by using the equation: 1) $FRET^c = FRET - (A \times FITC) - (B \times Cy3)$, where FRET, FITC, and Cy3 correspond to background-subtracted images of cells labeled with FITC- and Cy3-conjugated Abs acquired through the FRET, FITC, and Cy3 channels, respectively. Images of $FRET^c$ intensity were renormalized according to a lookup table, in which the minimum and maximum values are displayed as blue and red, respectively. Mean $FRET^c$ values were calculated from mean fluorescence intensities for each of the 10 regions of interest (ROI) selected from five different cells according to equation 1. $FRET^c$ values were related to the donor fluorophore (FITC), because CD6 expression is lower than that of CD43 in PBLs. Regions with high or low FITC:Cy3 ratios (i.e., outside the 1:1 to 1:4 stoichiometric range) were excluded from the analysis.

The apparent efficiency of FRET (E_a) was calculated according to the equation: 2) $E_a = FRET^c/FITC$, where $FRET^c$ and FITC are the mean intensities of $FRET^c$ and FITC in the selected ROI. These calculations allowed E_a to be <0. All calculations were performed using the Image Processing Leica Confocal Software and Microsoft Excel. The statistical analysis was performed by SPSS (Chicago, IL). The results are graphed showing the mean ± SD and percentiles 25 and 75. Statistical differences between groups were tested using the nonparametric Mann-Whitney *U* test. A value of $p < 0.001$ was taken to indicate statistical significance.

Expression of recombinant soluble proteins

The ectodomain of human CD5 (rsCD5) was expressed in HEK 293-EBNA by using an episomal expression system (26). The ectodomain of human CD6 (rsCD6) was essentially expressed in the same way. Briefly, the extracellular region of CD6 was PCR amplified by using the 5′-CT TCTAGATGACCAGCTCAACACCACCAGCA-3′ and 5′-GCGGATC CCTATTCTATAGTGACTGTCTGAACA-3′ primers and the CD6-PB1 cDNA (23) as a template. The PCR product was *Xba*I/*Bam*HI restricted and cloned into appropriately digested pCEP-Pu vector. The resulting construct was transfected into HEK 293-EBNA cells, as previously described (27, 28). The rsCD6 protein was affinity purified over CNBr-activated Sepharose 4B columns covalently coupled to 168.1 (anti-CD6) mAb. Biotinylation and cell-binding studies of rsCD5 and rsCD6 were conducted, as previously reported (26).

Conjugate formation analysis

Two types of T cell-APC conjugates were analyzed, namely Jurkat-Raji cells and primary T cells-dendritic cells (DC). The use of the Vβ8 TCR-expressing Jurkat cell (J77c120) and the human B line Raji has been reported elsewhere (29). Monocyte-derived DC were generated, as described (30). Briefly, peripheral blood monocytes were isolated and cultured for 5 days in the presence of IL-4 (R&D Systems, Minneapolis, MN) and GM-CSF (R&D Systems) (10 ng/ml and 1000 U/ml, respectively). Then LPS (10 ng/ml) (Sigma-Aldrich) was added for 36 h to the culture medium. The phenotype of mature DC was confirmed to be $CD1a^{high}$, $CD14^{low}$, and $CD83^{high}$ by flow cytometry analysis. Polyclonal SEB-specific primary T cells were generated, as described elsewhere (31). The S3085B (S3) T cell clone was generated by limiting dilution of polyclonal SEB-specific T cells.

Mature DC or Raji cells were incubated for 20 min at 37°C with 1 μg/ml SEB or 2 μg/ml SEE, respectively. In some experiments, Raji cells were also incubated with the cell tracker chloromethyl derivative of aminocoumarin. S3 T cells were mixed with DC, and J77 cells with Raji cells (5×10^4 cells), and then incubated for 15 min at 37°C. S3-DC cell mixture was plated onto fibronectin (20 μg/ml)-coated slides, and J77-Raji cell mixture was plated onto PLL (50 μg/ml)-coated slides, and incubated for 10–30 min at 37°C. Next, cells were fixed for 5 min with 4% formaldehyde in HBSS. For immunofluorescence assays, nonspecific binding sites were blocked with TNB (0.1 M Tris-HCL, 0.15 M NaCl, 0.5% blocking reagent; Boehringer Mannheim) and human γ-globulins (100 μg/ml; Sigma-Aldrich). Cell conjugates were saturated with mouse serum. Then cells were incubated either with MAE1-C10 (anti-CD6) or Leu-1 (anti-CD5) for 30 min at 37°C, followed by incubation with Alexa Fluor 488-labeled GAMIg (Molecular Probes) serum for additional 30 min. For double staining, cells were further incubated with biotinylated anti-ICAM-1 mAb plus Rhodamine Red X-SAv or, alternatively, permeabilized with 0.5% Triton X-100 for 2 min and then stained with rabbit polyclonal anti-CD3ζ serum plus Rhodamine Red-X-labeled goat anti-rabbit Ig serum. For double staining of ALCAM/CD166 and CD3, cells were incubated with a PE-conjugated anti-ALCAM/CD166 mAb, followed by a FITC-conjugated anti-CD3 mAb. S3-DC conjugates were examined with a DMR photomicroscope (Leica Microsystems), and images were acquired using the Leica QFISH 1.0 software. Series of optical sections of J77-Raji conjugates were obtained with a Leica TCS-SP confocal scanning laser microscope. Differential interference contrast (DIC) images were obtained.

Microtubule-organizing center (MTOC) translocation assays

For the inhibition of IS maturation, SEE-loaded Raji cells were preincubated with or without 10 μg/ml recombinant soluble proteins (rsCD6 or rsCD5). Then J77 T cells were added, and cell conjugates were prepared and fixed, as above. The cells were permeabilized for 1 min in PBS plus 1% Triton X-100 and then stained with anti-α-tubulin for 30 min at RT. Cell samples were visualized under confocal microscopy and scored for MTOC reorientation, considered as location of the MTOC in close proximity to the T cell plasma membrane, between the nucleus and the Raji contact region. We scored no more than 100 conjugates in each experiment.

Proliferation assays

Proliferation assays were conducted in triplicate wells of round-bottom 96-well plates (Costar, Corning, NY) for 4 days at 37°C in a humidified atmosphere of 5% CO_2 in air. Briefly, 1×10^5 PBL were cultured in a final volume of 200 μl of X-VIVO 10 (BioWhittaker, Verviers, Belgium) in the presence of 0.5 ng/ml OKT-3 (Ortho Biotech, Bridgewater, NJ), 0.125% PHA (Murex Biotech, Dartford, U.K.), or 5 μg/ml PWM (Sigma-Aldrich) alone or in combination with different concentrations (0.02–0.125 μM) of recombinant soluble purified proteins. Cells were labeled with [^{3}H]thymidine (Monavek Biochemicals, Brea, CA) for the last 16 h of culture, and were harvested using an automatic cell harvester. Results are presented as the mean and SD cpm.

Results

Coprecipitation of TCR/CD3 and CD6 from T lymphocytes

The TCR/CD3 complex is easily dissociated by detergent treatment. However, mild detergents such as digitonin or Brij 58 preserve its structure (32). Thus, the possible association of CD6 to the TCR/CD3 complex was explored by coimmunoprecipitation experiments of surface biotin-labeled T cells, solubilized under different detergent conditions (1% Brij 58, Brij 96, or Nonidet P-40). The presence of CD6 in CD5, CD3, and HLA class I immunoprecipitates from the HUT-78 T cell line was investigated by reprecipitation with a CD6-specific rabbit polyclonal antiserum. As shown in Fig. 1*A*, we detected the presence of CD6 in CD3 immunoprecipitates only when Brij 58 detergent cell solubilizates were used. In agreement with previous results (22), CD6 was also detected in CD5 immunoprecipitates from Brij 96 and Brij 58, but not Nonidet P-40 cell lysates. CD6 could not be detected in HLA class I immunoprecipitates under any of the detergent conditions used (Fig. 1*A*). Additional experiments performed on surface-biotinylated thymocytes and PBL under Brij 58 lysis conditions confirmed the presence of CD6 in CD3 immunoprecipitates from normal T cell types (Fig. 1*B*).

CD6 and TCR/CD3 association is independent of CD5

CD5 has been shown to associate with both TCR/CD3 (33) and CD6 (22, 34) under Brij 96-mediated cell membrane solubilization conditions. Thus, the possibility that the association of CD6 with TCR/CD3 was mediated by CD5 was investigated by coimmunoprecipitation assays on 2G5 cells, a $CD5^-CD6^-CD3^+$ Jurkat cell line derivative (16). A transfectant clone expressing a cytoplasmic tail-truncated CD6 protein ($CD6.A613^{stop}$) (Fig. 2*A*) was surface

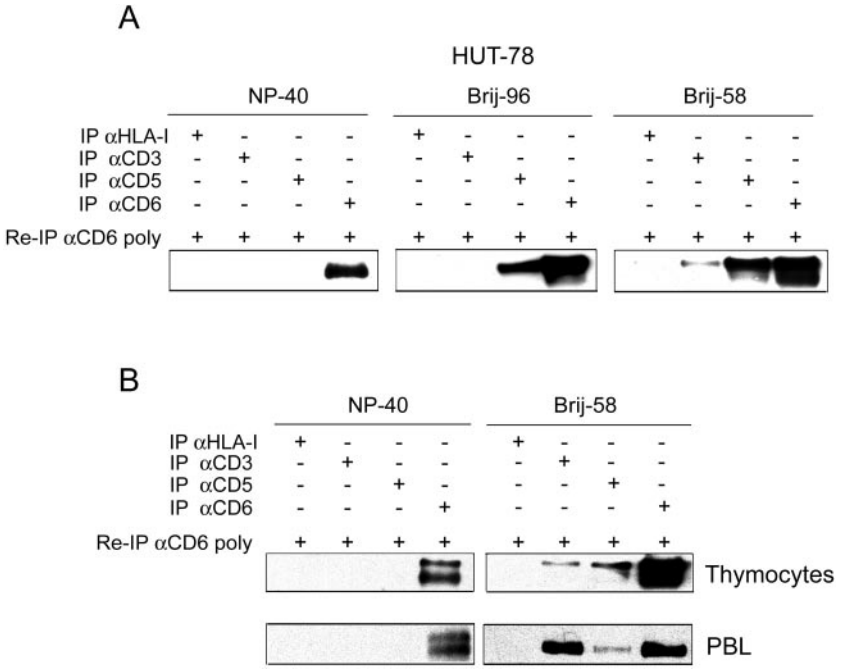

FIGURE 1. CD6 coprecipitates with CD3 from Brij 58 lysates of normal and leukemic human T cells. *A*, 25×10^6 HUT-78 cells were surface biotinylated and lysed with 1% Nonidet P-40, Brij 96, or Brij 58 lysis buffer. HLA class I, CD3-ϵ, CD5, and CD6 proteins were immunoprecipitated (IP) using specific mAbs (W6/32, 33-2A3, Cris-1, and 161.8, respectively) and reprecipitated (Re-Ip) with rabbit polyclonal antisera specific for CD6. Reprecipitates were run in 8% SDS-PAGE under reducing conditions and transferred to nitrocellulose. Biotinylated proteins were developed by HRP-SAv and ECL, followed by exposure to x-ray films. *B*, Thymocytes (2×10^8) and PBL (5×10^7) were surface biotinylated and lysed in either 1% Nonidet P-40 or Brij 58 lysis buffer and then analyzed, as described in *A*.

biotinylated and lysed under Brij 58 detergent conditions. HLA class I, CD3, CD5, and CD6.A613^{stop} molecules were immunoprecipitated with specific mAbs and reimmunoprecipitated with a rabbit polyclonal anti-CD6 antiserum. As shown in Fig. 2*A*, CD6.A613^{stop} was coimmunoprecipitated from CD3, but not HLA class I and CD5 immune complexes. These results indicate that not only CD5, but also the most C-terminal 55 aa of CD6 are dispensable for the association of CD6 with the TCR/CD3 complex.

Sequential immunodepletion assays further confirmed the CD5-independent association of CD6 with TCR/CD3. Surface biotin-labeled PBL were lysed with Brij 58 lysis buffer, and several rounds of immunoprecipitation with an anti-CD5 mAb removed CD5 molecules. CD5-depleted and undepleted lysates were then immunoprecipitated with anti-CD3 mAb, and the presence of CD6 or CD5 was investigated by reprecipitation with specific rabbit polyclonal antisera. As shown in Fig. 2*B*, the presence of bands corresponding to CD6 in CD3 immune complexes from both CD5-depleted and undepleted lysates was detected. This indicates that a portion of CD6 molecules associates with CD3 in a CD5-independent manner. As efficiency depletion control, the presence of CD5 was detected in CD3 immunoprecipitates from CD5-undepleted cells, but not in those from CD5-depleted cells (Fig. 2*B*).

TCR/CD3 partially cocaps with CD6 on T lymphocytes

To circumvent possible detergent-based artifacts as responsible for the coimmunoprecipitation of TCR/CD3 and CD6, we examined the ability of the two molecules to cocap using double immunofluorescence assays. Cocapping was explored by incubating PBL with biotin-labeled anti-CD6 mAb plus TR-labeled SAv for 30 min at 37°C, followed by fixation and staining with FITC-conjugated mAbs to either CD3 or CD43. As shown in Fig. 3*A*, partial cocapping of CD3 and CD6 was observed, thus supporting a possible physical association between them. The association was specific because another T cell surface molecule, CD43, showed little or no cocapping with CD6 (Fig. 3*A*).

FRET analysis of the CD6 and TCR/CD3 association

To further confirm that TCR/CD3 physically associate with CD6 on the lymphocyte surface, we performed FRET microscopy analysis, a method that can detect molecular proximity between two proteins with a resolution of tens of angstroms (25). Cy3-labeled mAb to CD3 was used as fluorescence acceptor, and FITC-conjugated mAb to CD6, CD5, and CD43 were used as donors. FRET measurements between CD6 and TCR/CD3 were performed on PBL under CD3-capping conditions and compared with those obtained for TCR/CD3 and CD43, two unrelated receptors used as background control, and for TCR/CD3 and CD5, two receptors known to be physically associated (positive control) (35). The FRET images obtained for the FITC anti-CD6/Cy3 anti-CD3, FITC anti-CD5/Cy3 anti-CD3, and FITC anti-CD43/Cy3 anti-CD3 mAb pairs used are shown in Fig. 3*B*. The efficiency of energy transference between FITC and Cy3 fluorochromes measured by calculating the sensitized FRET signal (FRET^c) on a pixel-by-pixel basis and the mean E_a values are also shown in Fig. 3*B*. Our results show that FRET at the CD3 cap is significantly higher for the CD3/CD6 pair than for the negative control CD3/CD43 pair, thus supporting a physical association between TCR/CD3 and CD6.

TCR/CD3 and CD6 colocalize at the cSMAC

The accumulation of CD6 at the IS (also named SMAC) under Ag T cell activation conditions has been recently reported (22). This finding was made using the Jurkat-Raji model of T-APC interaction. In this study, we have extended these observations to another in vitro model that uses primary T cells and DC (30). As shown in Fig. 4*A*, CD6 accumulated at the contact zone between polyclonal SEB-specific T cells and in vitro generated mature DC pulsed with SEB. This indicates that CD6 redistributes to the contact area between T-B and T-DC cell conjugates in an Ag-dependent manner.

To further investigate the precise location of CD6 at the IS, its relationship with ICAM-1 and TCR/CD3 molecules was assayed. As shown in Fig. 4*B*, CD6 accumulated at the cSMAC between J77 and Raji cells in the presence of SEE, while ICAM-1 remained at the pSMAC. The colocalization of CD6 with TCR/CD3 at the cSMAC is also shown (Fig. 4*B*). As expected, a similar localization at the cSMAC was observed for CD5 (Fig. 4*B*) (36). These

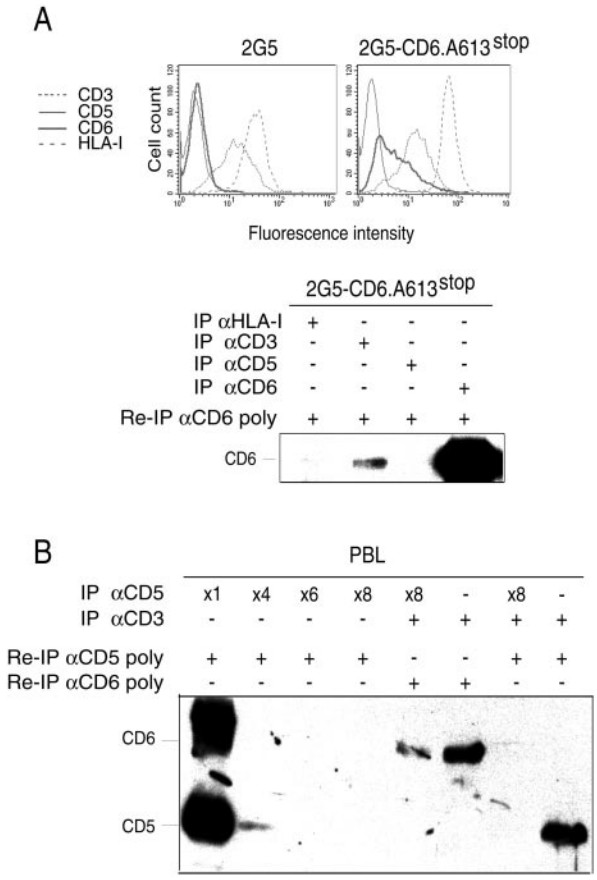

FIGURE 2. CD5-independent coprecipitation of CD6 and CD3. *A*, Specific coprecipitation of CD3 and CD6 molecules from CD5-deficient T cells. *Top*, Fluorescence histograms showing CD5, CD6, CD3ϵ, and HLA-I expression on 2G5 cells transfected or not with CD6.A613^{stop} construct. *Bottom*, Coprecipitation of CD6 and CD3 in the 2G5-CD6A613^{stop} cell transfectant. A total of 5×10^7 surface biotin-labeled cells was lysed in Brij 58 lysis buffer, and HLA class I, CD3ϵ, CD5, and CD6.A613^{stop} proteins were immunoprecipitated (IP) using specific mAbs (W6/32, 33-2A3, Cris-1, and 161.8, respectively). Then immune complexes were reprecipitated (Re-IP) with rabbit polyclonal anti-CD6 antiserum. Reprecipitates were run in 8% SDS-PAGE under reducing conditions and transferred to nitrocellulose. Biotinylated proteins were developed by HRP-SAv and chemiluminescence, followed by exposure to x-ray films. *B*, Coimmunoprecipitation of CD3 and CD6 from CD5-immunodepleted PBL lysates. Surface-biotinylated PBL (10×10^7) were lysed in 1% Brij 58 lysis buffer, split in two, and then subjected to several rounds (×1, ×4, ×6, ×8) of immunoprecipitation with anti-CD5 mAb (Cris-1). A second immunoprecipitation with anti-CD3 mAb (33-2A3) was conducted in the CD5-depleted and nondepleted samples. All of the immunoprecipitates were reprecipitated with rabbit polyclonal antisera to either CD6 or CD5 and developed as in *A*.

data indicate that when highly specialized and functionally relevant structures, such as IS, are formed, CD6 remains in close proximity to TCR/CD3, pointing out to a relevant role of CD6 in the modulation of TCR/CD3 signaling during T cell activation.

The localization of the CD6 ligand, ALCAM/CD166, within the IS topography was further analyzed in SEE-dependent Jurkat-Raji cell conjugates. As shown in Fig. 4*C*, double staining for CD3 and ALCAM/CD166 demonstrated that ALCAM/CD166 accumulates at the IS and colocalizes, at least partially, with TCR/CD3. The fact that only a fraction of ALCAM/CD166 molecules localizes at the cSMAC could be explained by the fact that ALCAM/CD166 not only interacts with CD6, but also mediates homophilic

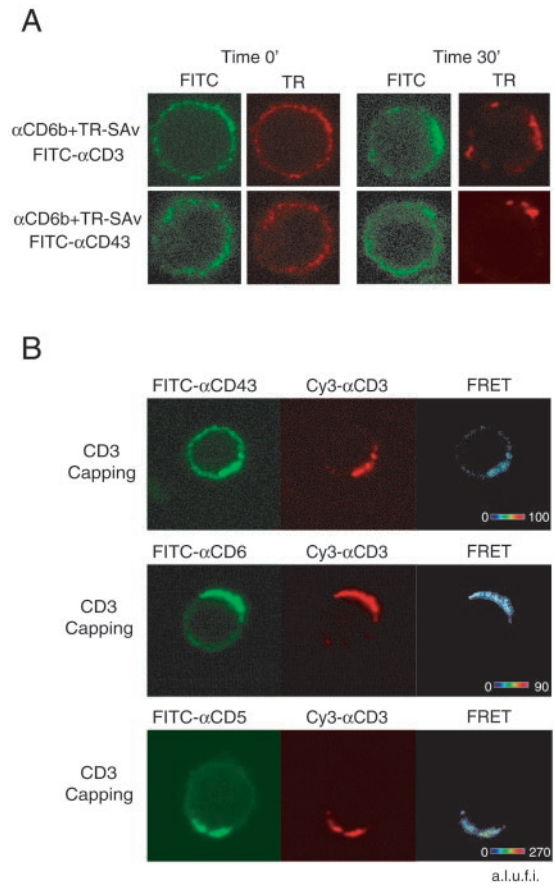

	Ea
FITC-αCD6/Cy3-αCD3	0,27
FITC-αCD43/Cy3-αCD3	0,14
FITC-αCD5/Cy3-αCD3	0,48

FIGURE 3. Analysis of CD3 and CD6 association by cocapping and FRET. *A*, PBL were induced to cap at 37°C with biotin-labeled anti-CD6 mAb (161.8) plus TR-SAv. At time 0 and 30 min, the cells were washed with ice-cold PBS/azide and stained with the indicated FITC-conjugated mAbs. The images show the red (TR) and green (FITC) fluorescence. *B*, FRET analysis of CD6 and CD3 association under capping conditions. PBL were induced to cap for 30 min at 37°C with Cy3-conjugated anti-CD3 mAb plus unlabeled GAMIg, and then stained with FITC-conjugated anti-CD6, anti-CD43, or anti-CD5 mAbs. FRET^c images were obtained, as described in *Material and Methods*, and presented as pseudocolor intensity-modulated images. A.l.u.f.i., Arbitrary linear units of fluorescence intensity. Bar, 2 μm. The apparent efficiencies of energy transference between FITC and Cy3, E_a, were calculated for several cell membrane regions (ROI). The mean E_a values ± SD are presented and graphed indicating the 25 and 75 percentiles. Asterisk indicates statistically significant difference ($p < 0.001$) as deduced from the Mann-Whitney *U* test. The mean E_a values are shown in the table.

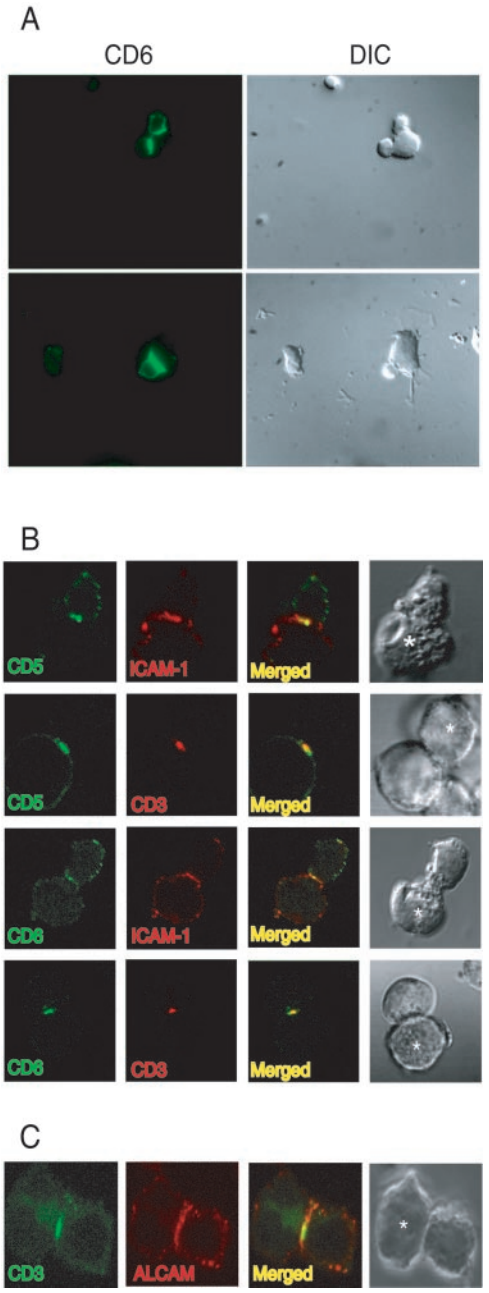

FIGURE 4. Distribution of CD6 and ALCAM at the mature IS. *A*, CD6 accumulates at the contact zone between DC and T lymphocytes. The S3 T cell clone was incubated with 1 μg/ml SEB and mixed with DC for 15 min at 37°C. Cell conjugates were allowed to adhere onto fibronectin-coated coverslips for 10 min, and then fixed and stained with anti-CD6 mAb (MAE1-C10) plus Alexa Fluor 488-labeled GAMIg. DIC images are shown. *B*, Colocalization of CD6 and CD3 at the cSMAC. Jurkat-Raji cell conjugates were incubated for 30 min in the presence of SEE and double stained for CD5 or CD6 (green) and ICAM-1 or CD3 (red). *C*, Localization of ALCAM at the IS. Jurkat-Raji cell conjugates were incubated for 30 min in the presence of SEE and double stained for ALCAM/CD166 (red) and CD3 (green). DIC images are shown. ∗, Raji cells.

ALCAM/CD166-ALCAM/CD166 interactions (37). Accordingly, ALCAM/CD166 was found expressed on Jurkat and Raji cells (data not shown).

Soluble CD6 inhibits IS maturation

The possible functional role of CD6-mediated interactions in T cell-mediated responses was addressed by assessing the effect of

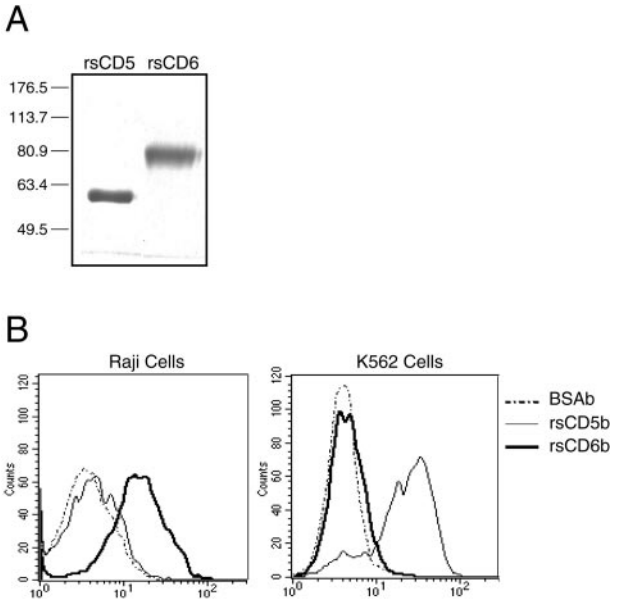

FIGURE 5. Analysis of purified rsCD5 and rsCD6 proteins. *A*, SDS-PAGE analysis. Affinity-purified rsCD5 and rsCD6 proteins were run into 10% SDS-PAGE under reducing conditions and stained by Coomassie blue. *B*, Cell-binding studies. Raji and K562 cells were incubated with biotinylated rsCD5, rsCD6, and BSA (rsCD5b, rsCD6b, and BSAb, respectively), and bond protein was detected with Tri-color-SAv.

rsCD6 on IS maturation. With this aim, rsCD6 was produced using a mammalian expression system and purified by affinity chromatography (Fig. 5*A*). rsCD5, a closely related member of the SRCR superfamily (8), was used as a control. The activity of the purified proteins was assessed by binding assays to cells expressing their respective counterreceptors (Fig. 5*B*) (21). Then SEE-loaded Raji cells were preincubated in the presence or absence of 10 μg/ml purified rsCD6 or rsCD5 and next mixed with J77 cells. Cell conjugates were stained for α-tubulin to detect MTOC reorientation, a marker of IS maturation. The presence of rsCD6 significantly reduced the MTOC reorientation, ranging from 30 to 47% (Table I). In contrast, no significant inhibitory effects were observed when cells were preincubated with rsCD5 (see Table I). Moreover, rsCD6 also reduced the number of cell contacts in which CD3 redistributed at the T-APC interaction site, an additional marker of mature IS (data not shown). Interestingly, the inhibitory effects of the rsCD6 on IS maturation were not seen when added 3 and 10 min after cell mixing, thus indicating that rsCD6 interferes with early cell-cell interactions needed for IS maturation to proceed (Table II).

Soluble CD6 inhibits T cell proliferation

The correct maturation of the IS is most likely required for optimal T cell activation and proliferation. We therefore investigated the ability of the rsCD6 protein to interfere with T cell proliferation. PBL were stimulated with optimal mitogenic concentrations of OKT-3 (0.5 ng/ml) mAb, PHA (0.125%), or PWM (5 μg/ml) in the presence or absence of increasing concentrations of recombinant soluble purified proteins (rsCD6 or rsCD5). As shown in Fig. 6, *A* and *B*, rsCD6 clearly inhibited both CD3- and PHA-mediated T cell proliferation in a dose-dependent manner. By contrast, rsCD5 induced dose-dependent inhibitory effects on CD3-mediated, but not on PHA-mediated T cell proliferation (Fig. 6, *A* and *B*). Possible toxic effects of rsCD5 and rsCD6 were ruled out by assessing cell viability by trypan blue dye exclusion and by observing noninhibitory effects on PWM-induced cell proliferation,

Table I. *Inhibitory effect of purified rsCD6 on the maturation of Ag-specific Raji-J77 cell conjugates*[a]

	Expt. 1		Expt. 2		Expt. 3	
Preincubation	% Mature IS	% Inhibition	% Mature IS	% Inhibition	% Mature IS	% Inhibition
—	64	0	67	0	70	0
Albumin	67	−4.6	61	8.9	ND	ND
rsCD5	62	3.1	60	10.4	61	12.8
rsCD6	40	37.5	36	46.2	40	42.2

[a] SEE-loaded Raji cells were preincubated or not with 10 μg/ml purified rsCD6 or rsCD5 before mixing with J77 cells. After 30 min of incubation, cells were stained with FITC-labeled anti-α-tubulin mAb. Raji-J77 cell conjugates were scored for the percentage of MTOC reorientation relative to the number of cell contacts counted (% mature IS). Raji cells were tracked with chloromethyl derivative of aminocoumarin. Here are shown the results of three independent experiments of six performed. The percentage of mature IS inhibition (% inhibition) was calculated, taking as 0 the percentage value of mature IS detected in the absence of recombinant proteins (−).

even at optimal inhibitory doses for either CD3- or PHA-induced proliferation (Fig. 6*C*). Similarly, we did not observe any inhibitory effect of either rsCD5 or rsCD6 on unidirectional or bidirectional MLR (data not shown). These data indicate that both rsCD5 and rsCD6 selectively inhibit T cell proliferation induced by certain stimuli, namely anti-CD3.

Discussion

The CD6 lymphocyte receptor was initially implicated in T cell activation as a costimulatory T cell molecule (9, 38). Later on, it was shown that CD6 specifically binds ALCAM/CD166, and that this interaction was responsible for thymocyte-thymic epithelial cell adhesion phenomena (13, 14). Extensive efforts to study the CD6-ALCAM/CD166 interaction showed that the membrane-proximal SRCR domain of CD6 (D3) binds to the most N-terminal Ig V-like domain of ALCAM/CD166 (V_1) (39, 40). Since then, few advances have been made on the precise biological effects of CD6-ligand interactions and signaling pathway of CD6. In the present study, we show that a fraction of CD6 molecules associates with the TCR/CD3 complex on normal and leukemic T cells. This physical relationship is maintained when specialized membrane structures, such as CD3 caps or Ag-induced SMAC, are formed. Accordingly, CD6 was shown to localize at the cSMAC. More importantly, the ability of rsCD6 to partially inhibit both IS maturation and T cell proliferation supports this notion. These data provide a physical basis for the previously reported role of CD6 both as a costimulatory and an adhesion molecule influencing T cell activation and differentiation processes (7).

The fact that CD6 and its ligand, ALCAM/CD166, occupy the cSMAC, in close proximity with the TCR/CD3 complex, has several biological implications. First, it supports the notion that the CD6-ALCAM/CD166 interaction plays an important role in T-APC interactions, most likely contributing to the formation and/or stabilization of the IS. The ability of rsCD6 to inhibit IS maturation at early stages supports this statement. Therefore, the CD6-ALCAM/CD166 pair should be considered as a relevant player among the lymphocyte receptors engaging nonpolymorphic ligands on professional APC and other cell types such as thymic epithelial cells. In the periphery, the CD6-ALCAM/CD166 interaction could contribute to the optimization of Ag-specific T-B, T-monocyte, and T-DC cell interactions. This is consistent with the previously reported monocyte-dependent costimulatory role of anti-CD6 mAbs on PBLs (9), as well as with the herein reported inhibition of CD3- and PHA-mediated T cell proliferation induced by rsCD6. In the thymus, the CD6-ALCAM/CD166 interaction most likely contributes to the differentiation process of thymocytes driven by resident epithelial and monocytic cells. In fact, CD6 expression correlates with thymocyte-positive selection and resistance to apoptosis (15). CD6 possesses a long cytoplasmic domain well suited for signal transduction (23), but the intracellular consequences of CD6 engagement by its ligand are mostly unknown. It has been shown, however, that TCR/CD3 stimulation induces tyrosine phosphorylation of CD6 (11, 12), which might then promote recruitment of signaling molecules and contribute to building the IS. The study of the signal transduction machinery recruited by CD6 will help to understand its costimulatory role during lymphocyte activation and differentiation processes.

Table II. *Effect of rsCD6 addition at different time points on IS maturation*[a]

	T0′ (%)	T3′ (%)	T10′ (%)
rsCD6	54	76	71
rsCD5	76	66	66

[a] Purified rsCD6 or rsCD5 (10 μg/ml) was added to SEE-loaded Raji cells before mixing with J77 cells (T0′) or at 3 (T3′) and 10 (T10′) min postmixing. After 30 min of incubation, cells were stained with FITC-labeled anti-α-tubulin mAb. Raji-J77 cell conjugates were scored for MTOC reorientation by visualization of fluorescence images. Raji cells were tracked with chloromethyl derivative of aminocoumarin. The data show the percentage (%) of mature IS.

The localization of CD6 and ALCAM/CD166 at the cSMAC indicates that the distance spanned by the interaction between CD6 and ALCAM/CD166 must be similar to that spanned by the TCR-MHC interaction. Otherwise, it would be physically impossible for the CD6-ALCAM/CD166 pair to redistribute and to colocalize with TCR/CD3 at the cSMAC. The current model of CD6-ALCAM/CD166 interaction, in which the ALCAM.V_1 domain embraces the CD6.D3 domain (39−41), is compatible with that assumption. Crystallography studies on the CD6-ALCAM/CD166 receptor-ligand complex are yet to be done, which will allow a better understanding of the physical basis of the interaction.

The physical relationship between CD6 and TCR/CD3 might have important consequences on the avidity of the CD6-ALCAM/CD166 interaction, as reported for other adhesion molecules, namely integrins. The kinetics of the CD6-ALCAM/CD166 interaction has been analyzed by surface plasmon resonance (41−43). Recent data indicate that the CD6-ALCAM/CD166 interaction is of low affinity (41) like most other leukocyte membrane protein interactions, e.g., CD28/CD152-CD80/CD86 (44) or CD2-CD58 (45). These data reinforce the proposed role played by the CD6-ALCAM/CD166 interaction in cell adhesion processes, which are of relevance to the formation and further stabilization of the IS. It would be interesting to determine the possible existence of changes on the avidity of this interaction by inside-out signaling following engagement of the TCR/CD3 by a specific Ag.

The inhibitory effect observed for rsCD6 not only on IS maturation, but also on T cell proliferation suggests that the CD6-ALCAM/CD166 interaction is functionally relevant to T cell activation. Our data are in agreement with a recent report in which soluble monomeric CD6 and CD166 chimeras (CD6CD4d3 + 4,

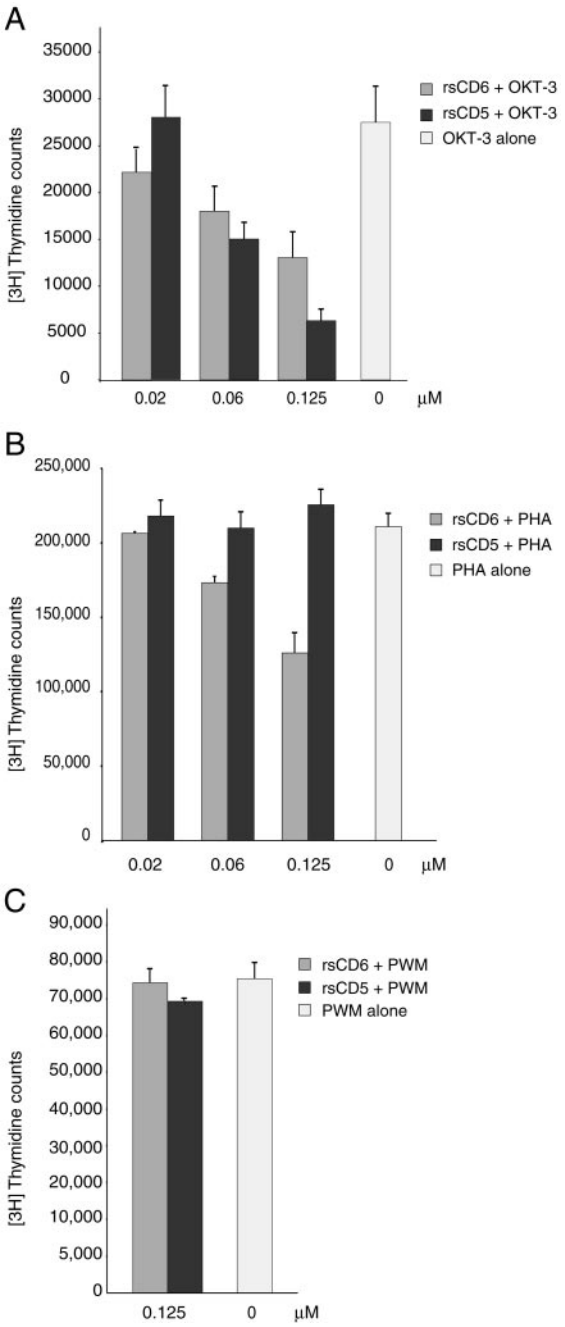

FIGURE 6. Inhibition of T cell proliferation by purified rsCD6. PBL were stimulated for 96 h with anti-CD3 mAb (OKT-3, 0.5 ng/ml) (*A*), PHA (0.125%) (*B*), or PWM (5 μg/ml) (*C*), in the presence or absence of different concentrations (0.02, 0.06, or 0.125 μM) of affinity-purified rsCD6 and rsCD5. The result of triplicate samples of a representative experiment of four independent experiments performed is shown. The mean and SD values of [^{3}H]thymidine counts are graphed.

and CD166CD4d3 + 4, respectively) were shown to inhibit cell proliferation induced by the tetanus toxoid Ag (41). We show in this study that the inhibition of T cell proliferative responses mediated by rsCD6 is, however, selective for only some of the stimuli used. It inhibited CD3- and PHA-induced cell proliferation, but not that induced by PWM or allogeneic cells. Intriguingly, we detected similar selective inhibitory effects for rsCD5. In this case, rsCD5 inhibited CD3-mediated T cell proliferation, but not that induced by PHA, PWM, or allogeneic cells. Although the effects of the rsCD6 on IS maturation and T cell proliferation are fully consistent, this is not the case for rsCD5. Apparently, rsCD5 inhibits T cell proliferation without interfering with IS maturation. One possible explanation is that rsCD5 may interfere with IS maturation at a level different from MTOC reorientation (e.g., tyrosine phosphorylation, protein kinase Cθ translocation). Another possibility is that the Raji cells used in our conjugate formation studies express low or absent CD5 ligand levels (Fig. 5*B*). Whatever the case, our data indicate that both CD5 and CD6 molecules are important signal-transducing molecules necessary for optimal TCR/CD3-mediated T cell activation. The release of soluble CD5 and CD6 could be, therefore, a physiological mechanism to either down-regulate or prevent lymphocyte activation. In fact, the presence of soluble CD5 and CD6 on serum from normal donors has been previously reported (46). Interestingly, the circulating levels of soluble CD5 and CD6 are higher in patients suffering from primary Sjögren's syndrome (46), a disorder that shows enhanced lymphocyte activation.

ALCAM/CD166 has also been implicated in homophilic interactions (37). These interactions are mediated through the membrane-distal V_1 domain of ALCAM/CD166 (37), which is also the domain involved in the heterophilic CD6-ALCAM/CD166 interaction. Therefore, the inhibitory effects shown for rsCD6 on IS maturation and T cell proliferation could be, at least in part, the result of interfering homophilic ALCAM/CD166 interactions. However, it has been shown that the homophilic interaction has 100-fold lower affinity than that of the heterophilic interaction (41), thus likely contributing to a lesser extent to cell-cell interactions. It also remains to be shown whether the homo- and heterophilic interactions mediated by the ALCAM.V_1 domain involve the same binding residues. The fact that the anti-ALCAM mAb J4-81 blocks heterophilic CD6-ALCAM/CD166 interactions (40) while increasing homotypic cell clustering of ALCAM$^+$CD6$^-$ cells (37) argues against that possibility. Nevertheless, recent binding competition studies indicate that the homophilic and heterophilic binding sites of ALCAM/CD166 are identical or at least overlapping (41).

In summary, the present study highlights the important role played by the molecular interactions mediated by CD6 during T cell activation and proliferation processes. This might result, at least in part, from its physical association with TCR/CD3. It seems very likely that cross talk events between these two surface receptors may contribute to the optimization of T cell activation and differentiation processes. Further work is needed to fully understand the underlying molecular mechanisms. Similarly, much effort is needed to better understand the functional consequences of the CD6-ALCAM/CD166 interaction. These studies would provide new clues on the cell interactions taking place not only during Ag presentation, but also during other cell-cell-mediated processes, such as those involved in the development of thymocytes or hemopoietic stem cells (47, 48).

Acknowledgments

We thank Dr. José Alberola-Ila for critical reading and reviewing of the manuscript, and Dr. Montserrat Plana and Dr. Teresa Gallart for help and advice.

References

1. Iezzi, G., K. Karjalainen, and A. Lanzavecchia. 1998. The duration of antigenic stimulation determines the fate of naive and effector T cells. *Immunity 8:89.*
2. Bromley, S. K., W. R. Burack, K. G. Johnson, K. Somersalo, T. N. Sims, C. Sumen, M. M. Davis, A. S. Shaw, P. M. Allen, and M. L. Dustin. 2001. The immunological synapse. *Annu. Rev. Immunol. 19:375.*
3. Monks, C. R., B. A. Freiberg, H. Kupfer, N. Sciaky, and A. Kupfer. 1998. Three-dimensional segregation of supramolecular activation clusters in T cells. *Nature 395:82.*
4. Dustin, M. L., M. W. Olszowy, A. D. Holdorf, J. Li, S. Bromley, N. Desai, P. Widder, F. Rosenberger, P. A. van der Merwe, P. M. Allen, and A. S. Shaw.

1998. A novel adaptor protein orchestrates receptor patterning and cytoskeletal polarity in T-cell contacts. *Cell 94:667*.

5. Dustin, M. L., and J. A. Cooper. 2000. The immunological synapse and the actin cytoskeleton: molecular hardware for T cell signaling. *Nat. Immunol. 1:23*.
6. Bowen, M. A., A. A. Aruffo, and J. Bajorath. 2000. Cell surface receptors and their ligands: in vitro analysis of CD6-CD166 interactions. *Proteins 40:420*.
7. Aruffo, A., M. A. Bowen, D. D. Patel, B. F. Haynes, G. C. Starling, J. A. Gebe, and J. Bajorath. 1997. CD6-ligand interactions: a paradigm for SRCR domain function? *Immunol. Today 18:498*.
8. Sarrias, M. R., J. Gronlund, O. Padilla, J. Madsen, U. Holmskov, and F. Lozano. 2004. The scavenger receptor cysteine-rich (SRCR) domain: an ancient and highly conserved protein module of the innate immune system. *Crit. Rev. Immunol. 24:1*.
9. Gangemi, R. M., J. A. Swack, D. M. Gaviria, and P. L. Romain. 1989. Anti-T12, an anti-CD6 monoclonal antibody, can activate human T lymphocytes. *J. Immunol. 143:2439*.
10. Osorio, L. M., M. Rottenberg, M. Jondal, and S. C. Chow. 1998. Simultaneous cross-linking of CD6 and CD28 induces cell proliferation in resting T cells. *Immunology 93:358*.
11. Wee, S., G. L. Schieven, J. M. Kirihara, T. T. Tsu, J. A. Ledbetter, and A. Aruffo. 1993. Tyrosine phosphorylation of CD6 by stimulation of CD3: augmentation by the CD4 and CD2 coreceptors. *J. Exp. Med. 177:219*.
12. Kobarg, J., G. S. Whitney, D. Palmer, A. Aruffo, and M. A. Bowen. 1997. Analysis of the tyrosine phosphorylation and calcium fluxing of human CD6 isoforms with different cytoplasmatic domains. *Eur. J. Immunol. 27:2971*.
13. Patel, D. D., S. F. Wee, L. P. Whichard, M. A. Bowen, J. M. Pesando, A. Aruffo, and B. F. Haynes. 1995. Identification and characterization of a 100-kD ligand for CD6 on human thymic epithelial cells. *J. Exp. Med. 181:1563*.
14. Bowen, M. A., D. D. Patel, X. Li, B. Modrell, A. R. Malacko, W. C. Wang, H. Marquardt, M. Neubauer, J. M. Pesando, U. Francke, et al. 1995. Cloning, mapping, and characterization of activated leukocyte-cell adhesion molecule (ALCAM), a CD6 ligand. *J. Exp. Med. 181:2213*.
15. Singer, N. G., D. A. Fox, T. M. Haqqi, L. Beretta, J. S. Endres, S. Prohaska, J. R. Parnes, J. Bromberg, and R. M. Sramkoski. 2002. CD6: expression during development, apoptosis and selection of human and mouse thymocytes. *Int. Immunol. 14:585*.
16. Simarro, M., C. Pelassy, J. Calvo, L. Places, C. Aussel, and F. Lozano. 1997. The cytoplasmic domain of CD5 mediates both TCR/CD3-dependent and -independent diacylglycerol production. *J. Immunol. 159:4307*.
17. San Jose, E., A. Borroto, F. Niedergang, A. Alcover, and B. Alarcon. 2000. Triggering the TCR complex causes the down-regulation of nonengaged receptors by a signal transduction-dependent mechanism. *Immunity 12:161*.
18. Luscinskas, F. W., G. S. Kansas, H. Ding, P. Pizcueta, B. E. Schleiffenbaum, T. F. Tedder, and M. A. Gimbrone, Jr. 1994. Monocyte rolling, arrest and spreading on IL-4-activated vascular endothelium under flow is mediated via sequential action of L-selectin, β_1-integrins, and β_2-integrins. *J. Cell Biol. 125:1417*.
19. Cardenas, L., A. C. Carrera, E. Yague, R. Pulido, F. Sanchez-Madrid, and M. O. de Landazuri. 1990. Phosphorylation-Dephosphorylation of the CD6 glycoprotein renders two isoforms of 130 and 105 kilodaltons: effect of serum and protein kinase C activators. *J. Immunol. 145:1450*.
20. Goding, J. W. 1976. Conjugation of antibodies with fluorochromes: modifications to the standard methods. *J. Immunol. Methods 13:215*.
21. Calvo, J., L. Places, G. Espinosa, O. Padilla, J. M. Vila, N. Villamor, M. Ingelmo, T. Gallart, J. Vives, J. Font, and F. Lozano. 1999. Identification of a natural soluble form of human CD5. *Tissue Antigens 54:128*.
22. Gimferrer, I., M. Farnos, M. Calvo, M. Mittelbrunn, C. Enrich, F. Sanchez-Madrid, J. Vives, and F. Lozano. 2003. The accessory molecules CD5 and CD6 associate on the membrane of lymphoid T cells. *J. Biol. Chem. 278:8564*.
23. Robinson, W. H., H. E. Neuman de Vegvar, S. S. Prohaska, J. W. Rhee, and J. R. Parnes. 1995. Human CD6 possesses a large, alternatively spliced cytoplasmic domain. *Eur. J. Immunol. 25:2765*.
24. Sorkin, A., M. McClure, F. Huang, and R. Carter. 2000. Interaction of EGF receptor and *grb2* in living cells visualized by fluorescence resonance energy transfer (FRET) microscopy. *Curr. Biol. 10:1395*.
25. Gordon, G. W., G. Berry, X. H. Liang, B. Levine, and B. Herman. 1998. Quantitative fluorescence resonance energy transfer measurements using fluorescence microscopy. *Biophys. J. 74:2702*.
26. Sarrias, M. R., O. Padilla, Y. Monreal, M. Carrascal, J. Abian, J. Vives, J. Yelamos, and F. Lozano. 2004. Biochemical characterization of recombinant and circulating human Spα. *Tissue Antigens 63:335*.
27. Kohfeldt, E., P. Maurer, C. Vannahme, and R. Timpl. 1997. Properties of the extracellular calcium binding module of the proteoglycan testican. *FEBS Lett. 414:557*.
28. Nischt, R., J. Pottgiesser, T. Krieg, U. Mayer, M. Aumailley, and R. Timpl. 1991. Recombinant expression and properties of the human calcium-binding extracellular matrix protein BM-40. *Eur. J. Biochem. 200:529*.
29. Niedergang, F., A. Dautry-Varsat, and A. Alcover. 1997. Peptide antigen or superantigen-induced down-regulation of TCRs involves both stimulated and unstimulated receptors. *J. Immunol. 159:1703*.
30. Romani, N., S. Gruner, D. Brang, E. Kampgen, A. Lenz, B. Trockenbacher, G. Konwalinka, P. O. Fritsch, R. M. Steinman, and G. Schuler. 1994. Proliferating dendritic cell progenitors in human blood. *J. Exp. Med. 180:83*.
31. Montoya, M. C., D. Sancho, G. Bonello, Y. Collette, C. Langlet, H. T. He, P. Aparicio, A. Alcover, D. Olive, and F. Sanchez-Madrid. 2002. Role of ICAM-3 in the initial interaction of T lymphocytes and APCs. *Nat. Immunol. 3:159*.
32. Cerny, J., H. Stockinger, and V. Horejsi. 1996. Noncovalent associations of T lymphocyte surface proteins. *Eur. J. Immunol. 26:2335*.
33. Beyers, A. D., L. L. Spruyt, and A. F. Williams. 1992. Molecular associations between the T-lymphocyte antigen receptor complex and the surface antigens CD2, CD4, or CD8 and CD5. *Proc. Natl. Acad. Sci. USA 89:2945*.
34. Castro, M. A., R. J. Nunes, M. I. Oliveira, P. A. Tavares, C. Simoes, J. R. Parnes, A. Moreira, and A. M. Carmo. 2003. OX52 is the rat homologue of CD6: evidence for an effector function in the regulation of CD5 phosphorylation. *J. Leukocyte Biol. 73:183*.
35. Osman, N., A. I. Lazarovits, and M. J. Crumpton. 1993. Physical association of CD5 and the T cell receptor/CD3 antigen complex on the surface of human T lymphocytes. *Eur. J. Immunol. 23:1173*.
36. Brossard, C., M. Semichon, A. Trautmann, and G. Bismuth. 2003. CD5 inhibits signaling at the immunological synapse without impairing its formation. *J. Immunol. 170:4623*.
37. Van Kempen, L. C., J. M. Nelissen, W. G. Degen, R. Torensma, U. H. Weidle, H. P. Bloemers, C. G. Figdor, and G. W. Swart. 2001. Molecular basis for the homophilic activated leukocyte cell adhesion molecule (ALCAM)-ALCAM interaction. *J. Biol. Chem. 276:25783*.
38. Morimoto, C., C. E. Rudd, N. L. Letvin, M. Hagan, and S. F. Schlossman. 1988. 2H1: a novel antigen involved in T lymphocyte triggering. *J. Immunol. 140:2165*.
39. Whitney, G. S., G. C. Starling, M. A. Bowen, B. Modrell, A. W. Siadak, and A. Aruffo. 1995. The membrane-proximal scavenger receptor cysteine-rich domain of CD6 contains the activated leukocyte cell adhesion molecule binding site. *J. Biol. Chem. 270:18187*.
40. Bowen, M. A., J. Bajorath, A. W. Siadak, B. Modrell, A. R. Malacko, H. Marquardt, S. G. Nadler, and A. Aruffo. 1996. The amino-terminal immunoglobulin-like domain of activated leukocyte cell adhesion molecule binds specifically to the membrane-proximal scavenger receptor cysteine-rich domain of CD6 with a 1:1 stoichiometry. *J. Biol. Chem. 271:17390*.
41. Hassan, N. J., A. N. Barclay, and M. H. Brown. 2004. Optimal T cell activation requires the engagement of CD6 and CD166. *Eur. J. Immunol. 34:930*.
42. Skonier, J. E., M. A. Bowen, J. Emswiler, A. Aruffo, and J. Bajorath. 1996. Mutational analysis of the CD6 binding site in activated leukocyte cell adhesion molecule. *Biochemistry 35:14743*.
43. Skonier, J. E., D. L. Bodian, J. Emswiler, M. A. Bowen, A. Aruffo, and J. Bajorath. 1997. Mutational analysis of the CD6 ligand binding domain. *Protein Eng. 10:943*.
44. Van der Merwe, P. A., D. L. Bodian, S. Daenke, P. Linsley, and S. J. Davis. 1997. CD80 (B7-1) binds both CD28 and CTLA-4 with a low affinity and very fast kinetics. *J. Exp. Med. 185:393*.
45. Van der Merwe, P. A., A. N. Barclay, D. W. Mason, E. A. Davies, B. P. Morgan, M. Tone, A. K. Krishnam, C. Ianelli, and S. J. Davis. 1994. Human cell-adhesion molecule CD2 binds CD58 (LFA-3) with a very low affinity and an extremely fast dissociation rate but does not bind CD48 or CD59. *Biochemistry 33:10149*.
46. Ramos-Casals, M., J. Font, M. Garcia-Carrasco, J. Calvo, L. Places, O. Padilla, R. Cervera, M. A. Bowen, F. Lozano, and M. Ingelmo. 2001. High circulating levels of soluble scavenger receptors (sCD5 and sCD6) in patients with primary Sjogren's syndrome. *Rheumatology 40:1056*.
47. Cortes, F., F. Deschaseaux, N. Uchida, M. C. Labastie, A. M. Friera, D. He, P. Charbord, and B. Peault. 1999. HCA, an immunoglobulin-like adhesion molecule present on the earliest human hematopoietic precursor cells, is also expressed by stromal cells in blood-forming tissues. *Blood 93:826*.
48. Ohneda, O., K. Ohneda, F. Arai, J. Lee, T. Miyamoto, Y. Fukushima, D. Dowbenko, L. A. Lasky, and T. Suda. 2001. ALCAM (CD166): its role in hematopoietic and endothelial development. *Blood 98:2134*.